Pure Appl. Chem., Vol. 82, No. 4, pp. 1045–1053, 2010.
doi:10.1351/PAC-CON-09-10-05

Optical and electrical properties of π-conjugated polymers built with the 10 π-electron methano[10]annulene ring system*

Patricia A. Peart, Giselle A. Elbaz, and John D. Tovar‡

Department of Chemistry, Johns Hopkins University, 3400 North Charles Street (NCB 316), Baltimore, MD 21218, USA

Abstract: Nontraditional aromatic molecules hold tremendous promise for the design and realization of advanced materials for organic electronics applications. In this report, we describe recent work with the 10 π-electron methano[10]annulene molecule. We used chemistry established by Vogel and by Neidlein to incorporate this molecule into organic semiconducting polymers and found that they provide for highly delocalized charge carriers upon electrochemical oxidation/doping into conductive materials. Extensions to a variety of annulene-heteroaromatic copolymers will be described along with pertinent optical and electrical characterization data.

Keywords: annulenes; aromaticity; conjugated polymers; cyclic voltammetry; spectroelectrochemistry.

INTRODUCTION

Aromaticity plays a crucial role in the performance of π-conjugated organic semiconductors and conducting polymers [1]. The nature of the quadrupole moments that exist within the constituent aromatic building blocks influences solid-state intermolecular interactions as evidenced in the diverse scope of π-stacking interactions within single crystals or as thermally deposited thin films of organic π-electron materials. These π-stacking interactions ultimately dictate the extent of intermolecular charge transport within the solid-state materials. Aromaticity also influences the intrapolymer delocalization of charge within a given polymer backbone. The effective conjugation length (ECL) of a conjugated polymer depends in part on the extent to which the π-electrons are delocalized, and it follows that components with greater aromatic resonance stabilization serve in essence to restrict this conjugation length. Likewise, the interplay of the aromatic and quinoidal resonance structures that exist within conjugated polymers is influenced by the energetic penalty that must be paid to break aromaticity in order to adopt an extended and highly conjugated quinoidal structure upon electrochemical oxidation of a given polyaromatic conjugated backbone [2,3]. These electronic considerations have been put into practice over the years to synthesize a variety of elaborate π-conjugated molecular and polymeric materials with robust electrical properties.

Pure Appl. Chem.* **82, 757–1063 (2010). An issue of reviews and research papers based on lectures presented at the 13th International Symposium on Novel Aromatic Compounds (ISNA-13), 19–24 July 2009, Luxembourg City, Luxembourg on the theme of aromaticity.
‡Corresponding author

A SURVEY OF METHANO[10]ANNULENE π-CONJUGATED COPOLYMERS

We recently embarked on a proof-of-principle re-examination of the 1,6-methano[10]annulene hydrocarbon made famous by the pioneering efforts of Vogel in the mid 1960s [4]. Much attention over the past four decades has focused on the molecular properties of this 10 π-electron monocyclic circuit. Under the umbrella of studying unusual aromatic components as polymeric π-electron materials [5], we wanted to merge the fascinating molecular properties of this structure into functional solid-state organic polymers. This was not only rooted in intellectual curiosity but with the fundamental electronic properties of the annulene. For example, the resonance stabilization of the annulene is lower than benzene [6], and its reactivity is notably olefinic in nature [7]. These facts suggested to us that the annulene may resemble a weakly aromatic "cyclic polyene", therefore lowering the energetic costs that must be paid to achieve highly delocalized quinoidal electronic structures. We describe here our recent characterization of the physical properties of annulene-based conducting polymers. Although these studies have been conducted in parallel with chemical syntheses of soluble polymers, we restrict our discussion here to analytical electrochemical work.

A comparative study of thiophene copolymers containing methano[10]annulene and naphthalene

Polymerizable π-conjugated monomers were synthesized via Stille couplings of 2,7-dibromo-1,6-methano[10]annulene with 2-tributylstannyl thiophene (to yield **MT**) or 5-tributylstannyl-2,2'-bithiophene (to yield **MBT**) [8,9], in a manner analogous to Neidlein's preparation of alkynylated annulenes using Sonogashira couplings [10]. Their naphthalene counterparts (**NT** and **NBT**) were synthesized in a similar manner starting from 1,5-diiodonaphthalene. Both central units have 10 π-electrons, but we hypothesized that the benzenoid nature of the fused acene would serve as an energetic barrier for extended delocalization relative to the annulene π-circuit. UV–vis measurements revealed that the annulene monomers had greater maximum wavelengths of absorption (λ_{max}) along with lower energy onsets of absorption relative to the naphthalene monomers (Fig. 1). These data suggest that greater delocalization can be achieved within the annulene-containing monomers, thereby encouraging a greater ECL which is the length of an oligomeric unit that has the same optical properties as the corresponding polymer. The λ_{max} values found for the annulene monomers are comparable to other more linearly conjugated π-electron molecules such as bithiophenes attached to 1,4-phenylenes (λ_{max} 391 nm) [11], or 2,5-thienylenes (λ_{max} 431 nm) [12]. This further reveals the delocalized nature of the annulene monomers despite the "Z-shaped" conjugation path imposed by the annulene in this particular configuration.

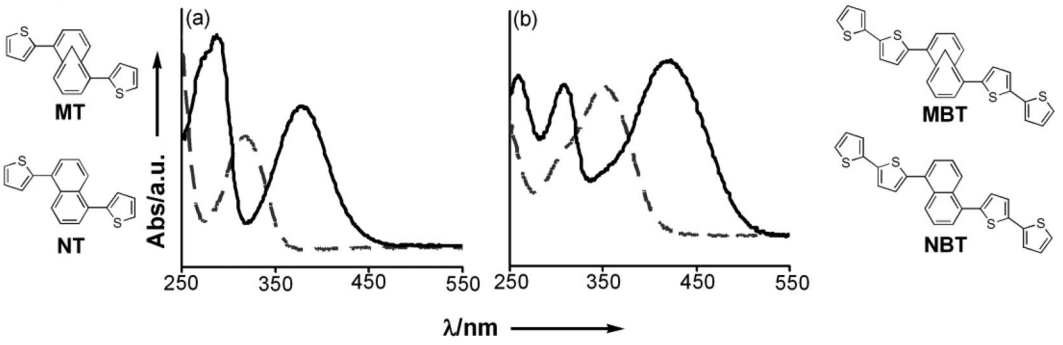

Fig. 1 UV–vis spectra of (a) **MT** (solid) and **NT** (dashed) and (b) **MBT** (solid) and **NBT** (dashed), taken in chloroform at room temperature. Extinction coefficients (λ_{max}, log ε): **MT** (284 nm, 4.52; 375 nm, 4.34), **NT** (315 nm, 4.27), **MBT** (257 nm, 4.52; 306 nm, 4.50; 416 nm, 4.57) and **NBT** (351 nm, 4.52).

The monomers were polymerized through electrochemical oxidation on platinum button electrodes. The annulene-containing monomers had lower oxidation potentials than their naphthalene counterparts reflecting their higher HOMO (highest occupied molecular orbital) levels. The destabilization of the HOMO (and the stabilization of the lowest unoccupied molecular orbital, LUMO) is expected as the π-electron framework becomes more conjugated. Lower monomer oxidation potentials are favorable since they reduce the possibility of polymer over-oxidation during electropolymerization. In addition, the monomer cyclic voltammetry (CV) for the annulenes indicated high degrees of electrochemical reversibility while those of their naphthalene counterparts showed irreversible behavior. For all monomers, the increase in the current of subsequent CV scans indicated the formation of electrode-bound electroactive species (Fig. 2). The relatively small increases along with the very thin films observed on the electrodes for the annulene-containing monomers indicated poor polymer growth. For **MT**, the more positive potential anodic peak corresponding to monomer oxidation decreases in intensity with continued scanning while the lower potential peak associated with polymer oxidation increases, most likely due to electrode surface passivation to some extent during polymer growth. The reversible electrochemical growth profiles of **MT** and **MBT** reflect the stability that methano[10]annulene core provides to the radical cations once formed. This stability also accounts for the sluggish polymer growth and the presumed formation of shorter polymer chains than those formed from naphthalene monomers.

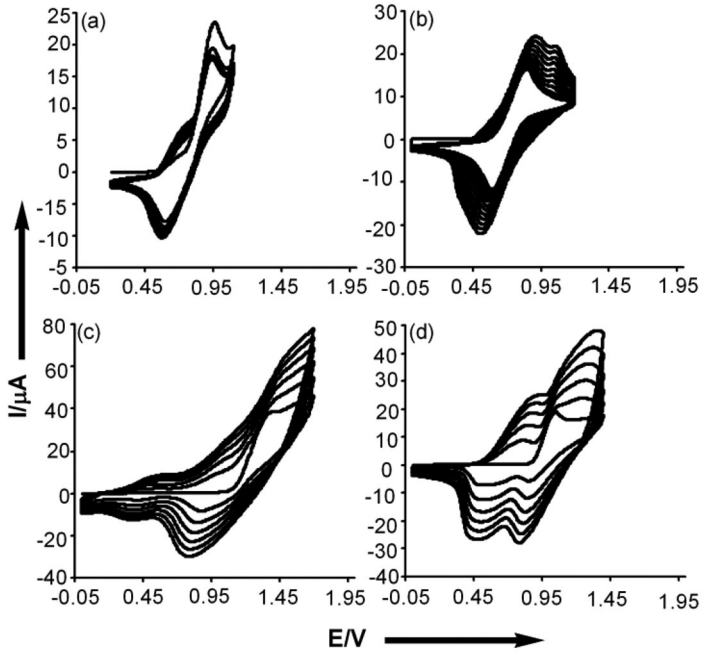

Fig. 2 Cyclic voltammetry for (a) **MT**, (b) **MBT**, (c) **NT** and (d) **NBT** at a 2 mm^2 Pt button electrode taken in solutions of 5 mM monomer and 0.1 M *n*-Bu_4NPF_6 in CH_2Cl_2. Potentials reported vs. a quasi-internal Ag/Ag^+ reference electrode, scan rate ν = 100 mV/s (modified from ref. [9] with permission. Copyright © 2008, Wiley-VCH Verlag GmbH & Co. KGaA).

The electrode-bound polymers were rinsed with monomer-free electrolyte and their CVs were recorded (Fig. 3). Polymers containing methano[10]annulene were easier to oxidize than their naphthalene counterparts, and they had CVs that were typical of conductive polymers and showed single oxidation peaks. Poly(**MT**) had the lowest oxidation potential among these four polymers which we spec-

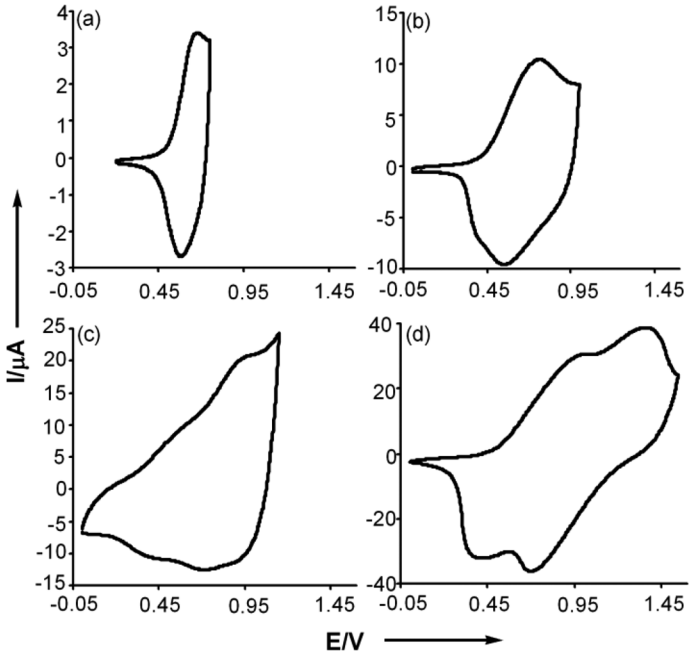

Fig. 3 Cyclic voltammetry for (a) poly(**MT**), (b) poly(**MBT**), (c) poly(**NT**), and (d) poly(**NBT**). Conditions as reported in Fig. 2 (modified from ref. [9] with permission. Copyright © 2008, Wiley-VCH Verlag GmbH & Co. KGaA).

ulate is due to the greater delocalization that can be achieved through the incorporation of a greater ratio of annulene units. In the other extreme, poly(**NBT**) displayed two clearly irreversible redox processes that could be due in part to poor conductivity within the localized electronic polymer, or due to surface packing effects that require an overpotential for anodic processes [13].

These polymers were electropolymerized onto transparent indium tin oxide (ITO) glass electrodes for the acquisition of UV–vis spectra while varying the potential applied to the polymer films (Fig. 4). Despite the possibility that the annulene polymers had shorter chain lengths than their naphthalene counterparts, they had higher λ_{max} values and lower energy onsets of absorption. We also noted broader neutral and polaronic peaks within the annulene-containing polymers that we attribute to the superposition of different active chromophores with differing conjugation lengths within the polymer. Much narrower peaks were observed for the naphthyl polymers, which points to them having shorter and more uniform ECLs as would be expected if delocalization only extends over a limited length of the polymer. One energetically reasonable scenario is where the stronger resonance stabilization in the naphthyl core restricts extended delocalization, in effect localizing the charge carriers to the oligothienyl segments or some other similarly defined molecular subunit. Since the conjugation lengths seem shorter to begin with in the naphthalene polymers, conformational disorder in the thin solid films would not make as dramatic of a difference when compared to the more delocalized annulene polymers. Additionally, for poly(**NBT**) a very clear isosbestic point was observed and this further supports the idea of more uniform ECLs as it resembles a molecular system with two defined absorbing species that are interconverted through a chemical process (such as between a neutral polymer and the charged radical cation of limited ECL). A very schematic depiction of this idea is presented in Fig. 5.

Qualitative in situ conductivity profiles of poly(**MT**) and poly(**MBT**) were measured on interdigitated Pt microelectrode arrays [14]. A 40 mV potential difference was maintained across the two microelectrodes during the CV experiment, and the potentials (V_G) of both electrodes were varied vs.

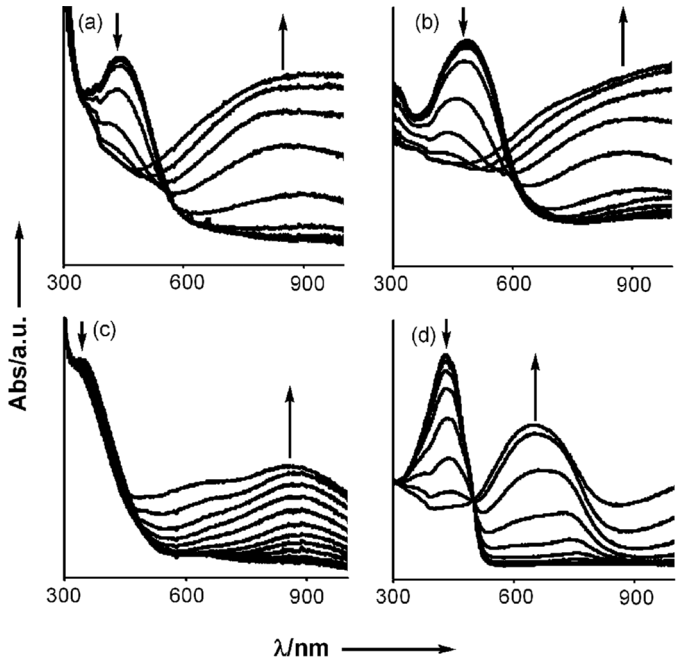

Fig. 4 Spectroelectrochemical data for (a) poly(**MT**), (b) poly(**MBT**), (c) poly(**NT**), and (d) poly(**NBT**) grown on ITO electrodes, with other conditions as reported in Fig. 2 (modified from ref. [9] with permission. Copyright © 2008, Wiley-VCH Verlag GmbH & Co. KGaA).

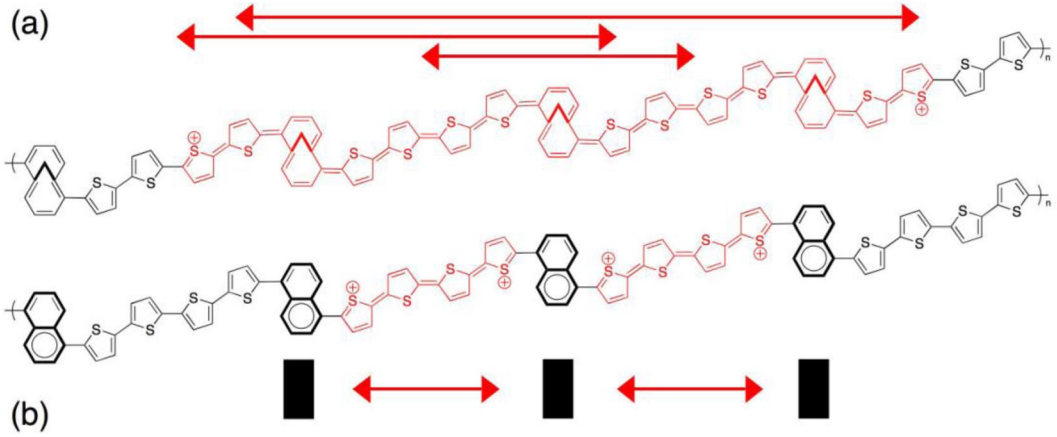

Fig. 5 Effective conjugation lengths of (a) the annulene polymers, where the maximum length may not be achieved since electrode packing may influence dihedral angles, thus leading to different absorbing chromophores, and (b) the naphthalene polymers, where the naphthalene serves as an energetic barrier for extended delocalization, thus restricting the conjugation length in the first place.

the reference electrode at the same scan rate. For a p-channel conductive polymer, a drain current (I_D) will flow between the two electrodes once the polymer has been oxidized into a conductive state. The magnitude of the current is directly proportional to the conductivity of the polymer. Therefore, plotting the graph of I_D vs. V_G gives relative conductivities at specific points of the polymer CV (Fig. 6). Poly(**MT**) was conductive between 0.50 and 0.90 V with its peak conductivity observed at 0.74 V.

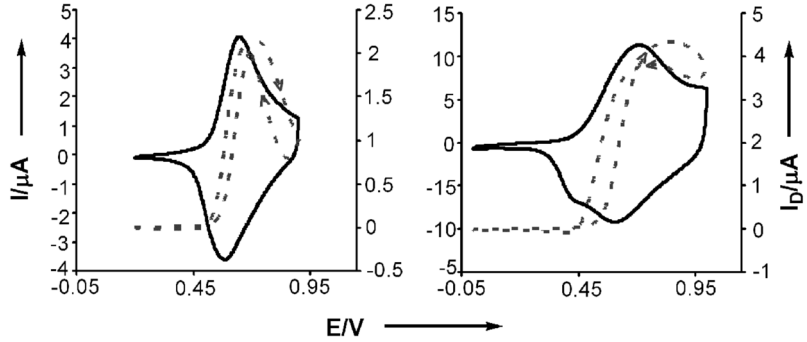

Fig. 6 Cyclic voltammetry (solid line) of poly(**MT**) (left) and poly(**MBT**) (right) as taken on Pt interdigitated microelectrode arrays and their in situ conductivity profiles obtained at 5 mV/s (dashed). Other conditions as reported in Fig. 2.

Poly(**MBT**) was conductive over a larger range, between 0.43 and 1.00 V with its peak conductivity observed at 0.82 V. Both polymers had a difference in the magnitude of the peak drain current between the forward and reverse scans as well as a slight hysteresis, observations usually attributed to film swelling or reorganization as solvent and electrolyte diffuse into the film to compensate for the charges on the oxidized polymers [15]. The peak intensity for each subsequent sweep decreased slightly for both polymers which suggests some degradation of the polymer during these measurements (done under ambient with very slow scan rates). CVs obtained under more typical conditions (ca. 100 mV/s) show stable and reproducible electroactivity.

One of the important practical considerations for any organic electronic material is its stability under ambient operating conditions. Polyacetylene, although highly conductive, is very susceptible to degradation in its oxidized state, but the annulene polymers are stable under ambient lab conditions employed for routine electrochemical measurements. We also studied the electrochemical reversibility within model monomer systems to gain insight as to the stability and robustness in the analogous polymers. The methyl-blocked version of the **MT** monomer (**Me-MT**) showed two distinct and electrochemically reversible redox processes with half-wave potentials of 0.71 and 0.89 V (Fig. 7). Despite the contributions of the cyclic polyene nature within the annulene core, we find that the **Me-MT** does not undergo follow-up reactivity or decomposition in its oxidized form, and we would expect the annulene in the copolymer to be similarly robust.

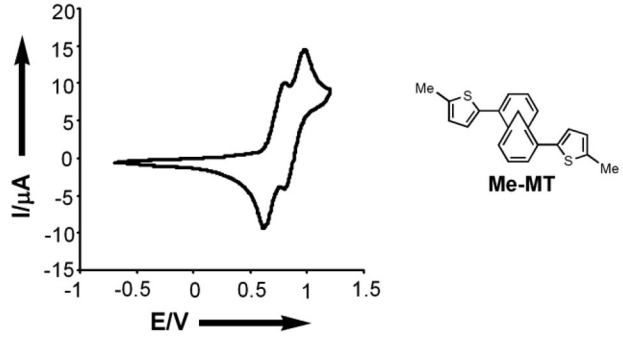

Fig. 7 Cyclic voltammetry of **Me-MT**. Conditions as reported in Fig. 2.

Furan copolymers containing methano[10]annulene

A series of furan-arene-furan monomers was synthesized to further investigate the viability of 1,6-methano[10]annulene as a building block for conductive organic polymers [16]. The furan motif was targeted due to the relative scarcity of functional furan-containing π-electron materials. Monomers where the arene was the prototypical aromatic benzene (**FBF**), the 10 π-electron naphthalene (**FNF**) and the methano[10]annulene (**FMF**) were studied in solution with UV–vis and were electropolymerized. The resulting polymers were investigated with UV–vis, CV, spectroelectrochemistry and in situ conductivity measurements. UV–vis spectra revealed that the **FMF** monomer has a greater λ_{max} than both **FBF** and **FNF** as well as a lower-energy onset of absorption (Fig. 8) in line with our prior results. This indicates that **FMF** has a greater extent of conjugation throughout the annulene core that results in a smaller HOMO–LUMO gap. Notably, **FMF** shows a substantial increase in λ_{max} despite the "Z-shape" conjugation pathway carved through the monomer.

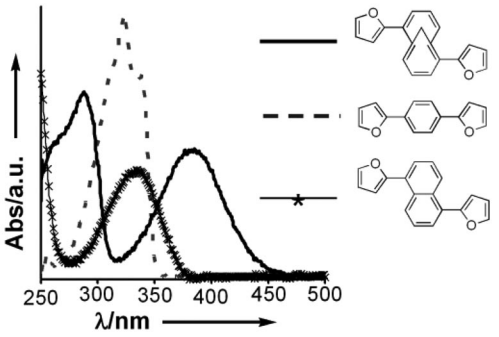

Fig. 8 UV–vis spectra for **FMF** (solid), **FBF** (dashed) and **FNF** (solid with cross markers) taken in chloroform at room temperature. Extinction coefficients (λ_{max}, log ε): **FMF** (287 nm, 4.43; 385 nm, 4.27), **FBF** (323 nm, 4.59), **FNF** (334 nm, 4.19).

The monomers were electropolymerized onto ITO-coated electrodes for spectroelectrochemical studies (Fig. 9). The λ_{max} of neutral poly(**FMF**) was shifted approximately 40 nm to the red compared to poly(**FBF**) and almost 100 nm longer than poly(**FNF**). The absorption peaks, both neutral and polaronic, of poly(**FMF**) were broader than those of poly(**FBF**) and poly(**FNF**), suggestive of superimposed absorbing chromophores within the polymer as discussed earlier. The poly(**FNF**) high energy peak persisted throughout the measurement suggestive of a localized electronic structure. Additionally, an isos-

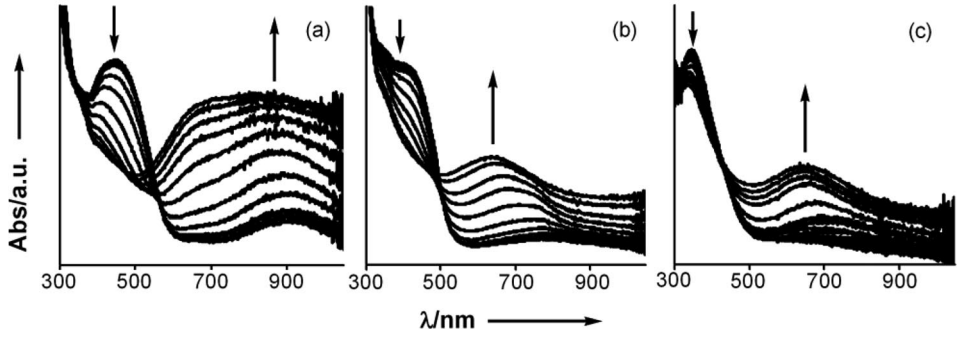

Fig. 9 Spectroelectrochemical data for (a) poly(**FMF**), (b) poly(**FBF**), and (c) poly(**FNF**) on ITO-coated glass electrodes, conditions as in Fig. 2.

bestic point was observed in the poly(**FBF**) and poly(**FNF**) spectra, which indicated some amount of electronic structure localization in the oxidized state. The broad absorption profile present in annulene-thiophene copolymers upon electrochemical oxidation was also found in poly(**FMF**).

Qualitative in situ conductivity measurements revealed windows of conductivity for both poly(**FBF**) and poly(**FMF**) as shown in Fig. 10. Poly(**FMF**) was conductive between the range of 0.25 and 0.65 V, with conductivity reaching a maximum at 0.50 V. The magnitude of the peak intensity decreased significantly with each subsequent sweep apparently due to some polymer degradation during the measurement. Poly(**FBF**) was conductive between the range of 0.28 and 0.75 V with its conductivity plateauing at 0.65 V. The magnitude of the peak intensity decreased only slightly with each subsequent sweep and suggests that there is little if any polymer degradation occurring. The **FNF** monomer polymerized very poorly on the devices used to determine conductivity, and we were unable to obtain comparative data for poly(**FNF**).

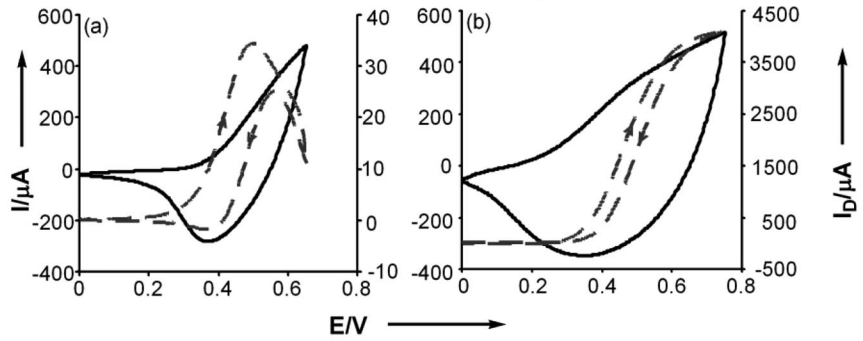

Fig. 10 Cyclic voltammograms (solid) and in situ conductivity profiles (dashed) of (a) poly(**FMF**) and (b) poly(**FBF**), taken on Au interdigitated electrodes with conditions as reported in Figs. 2 and 6.

CONCLUSIONS

Nontraditional π-electron molecules such as the methano[10]annulenes continue to play important roles to refine the concept of aromaticity as a fundamental molecular property. As aromatic molecules, it stands to reason that they should be equally valuable as components of π-conjugated oligomeric or polymeric materials. It seems that the synthetic complexities associated with these unusual aromatic molecules has hampered new investigations in this latter regard, and we hope that the explorations as summarized in this article will show that they are indeed viable substructures for highly delocalized and conductive organic electronic materials.

EXPERIMENTAL

CV was carried out using an Autolab PGSTAT302 potentiostat using 2 mm^2 platinum button (BioAnalytical Systems), ITO-coated glass (70–100 Ω/sq surface resistivity, Aldrich) or interdigitated working electrodes (Pt electrodes with 5 μm spacing from Abtech, #IME 0550.5 M, Pt, U; Au electrodes with 15 μm spacing from Microsensor Systems, #M1450110). Qualitative in situ conductivity was obtained using the above-mentioned instrument by utilizing the bipotentiostat settings. Polymers were electropolymerized on the microelectrode arrays from a 2.5 mM solution of monomer in 0.1 M *n*-Bu_4PF_6/CH_2Cl_2. The CV of the polymer was then recorded. Finally, drain current was measured within the same potential range as the CV was measured. A potential difference of 40 mV was applied between the two working electrodes, and both electrodes of the array were scanned at 5 mV/s. UV–vis spectra for spectroelectrochemical analysis were taken on a Cary 50 UV–vis spectrophotometer. More

detailed information can be found in our prior reports [8,9,16]. The synthesis of **Me-MT** was achieved in 94 % yield via Stille coupling between 2,7-dibromo-1,6-methano[10]annulene[17] (401 mg, 1.34 mmol) and 2-tributylstannyl-5-methylthiophene (1.298 g, 3.353 mmol) in DMF (10 ml) at 80 °C for 16 h in the presence of catalytic $Pd(PPh_3)_4$ (72 mg, 0.062 mmol) according to our previously reported methods. Representative characterization data for **Me-MT**: ^{1}H NMR (400 MHz, d_6-acetone) δ: 7.85 (d, J = 8.7 Hz, 2H), 7.40 (d, J = 9.6 Hz, 2H), 7.32 (d, J = 3.5 Hz, 2H), 7.15 (t, J = 9.4 Hz, 2H), 6.88 (m, 2H), 2.53 (s, 6H), –0.12 (s, 2H). ^{13}C NMR (100 MHz, $CDCl_3$) (δ: 141.4, 141.2, 135.4, 129.9, 127.9, 127.5, 127.1, 126.3, 118.1, 36.0, 15.7. HR-MS (EI): found m/z = 334.0850 [M^+]; calc. for $C_{21}H_{18}S_2$: 334.0850.

ACKNOWLEDGMENTS

Generous financial support was provided by Johns Hopkins University, the donors of the Petroleum Research Fund (45738-G7, administered by the American Chemical Society), and the National Science Foundation (CAREER, DMR-0644727). G.E. was the recipient of a Provost's Undergraduate Research Award (JHU).

REFERENCES

1. M. Kertesz, C. H. Choi, S. J. Yang. *Chem. Rev.* **105**, 3448 (2005).
2. J.-L. Brédas, G. B. Street. *Acc. Chem. Res*. **18**, 309 (1985).
3. A. O. Patil, A. J. Heeger, F. Wudl. *Chem. Rev*. **88**, 183 (1988).
4. E. Vogel, H. D. Roth. *Angew. Chem., Int. Ed.* **3**, 228 (1964).
5. E. L. Spitler, C. A. Johnson, M. M. Haley. *Chem. Rev.* **106**, 5344 (2006).
6. W. R. Roth, M. Bohm, H. W. Lennartz, E. Vogel. *Angew. Chem., Int. Ed. Engl*. **22**, 1007 (1983).
7. E. Vogel, W. A. Boll, M. Biskup. *Tetrahedron Lett.* 1569 (1966).
8. P. A. Peart, J. D. Tovar. *Org. Lett*. **9**, 3041 (2007).
9. P. A. Peart, L. M. Repka, J. D. Tovar. *Eur. J. Org. Chem*. 2193 (2008).
10. R. Neidlein, U. Kux. *Chem. Ber*. **127**, 1523 (1994).
11. T. Sato, K. Hori, M. Fujitsuka, A. Watanabe, O. Ito, K. Tanaka. *J. Chem. Soc., Faraday Trans.* **94**, 2355 (1998).
12. U. Mitschke, P. Bäuerle. *J. Chem. Soc., Perkin Trans. 1* 740 (2001).
13. A. Yassar, J. Roncali, F. Garnier. *Macromolecules* **22**, 804 (1989).
14. D. Ofer, R. M. Crooks, M. S. Wrighton. *J. Am. Chem. Soc*. **112**, 7869 (1990).
15. P. Audebert, F. Miomandre. In *Handbook of Conducting Polymers*, Vol. 1, 3rd ed., T. A. Skotheim, J. R. Reynolds (Eds.), p. 18.1, CRC Press, New York (2007).
16. P. A. Peart, J. D. Tovar. *Macromolecules* **42**, 4449 (2009).
17. E. Vogel, W. A. Böll. *Angew. Chem., Int. Ed*. **3**, 642 (1964).

